*Constants*; Chapman and Hall, 3rd ed. London, U. K., 1984; p 145.
15. Castro, E. A.; Ibanez, F.; Salas, M.; Santos, J. G. *J. Org. Chem.* **1991**, *56*, 4819.
16. Castro, E. A.; Salas, M.; Santos, J. G. *J. Org. Chem.* **1994**, *59*, 30.
17. Lee, I.; Koh, H. J.; Lee, B.-S.; Lee, H. W.; Choi, J. H. *Bull. Korean Chem. Soc.* **1990**, *11*, 435.
18. Guggenheim, E. A. *Phil. Mag.* **1926**, *2*, 538.

# Ultrahigh Vacuum Study for the Model Systems of Ziegler-Natta Catalyst

**Chang-Seop Ri**

*Department of Chemistry, Keimyung University, Taegu 704-701, Korea*
*Received March 10, 1995*

The surface structure of the adsorption site for the identification of active sites involved in the Ziegler-Natta catalyst was studied by surface science techniques. As an example of a real catalyst, $TiCl_3$ single crystals were prepared in a gradient furnace designed for this study and characterized by Auger Electron Spectroscopy (AES) and Low Energy Electron Diffraction (LEED) under ultrahigh vacuum condition. The chlorine covered Ti (0001) surface was employed as a model catalyst for the study of Ziegler-Natta catalyst. The diffuse LEED (DLEED) technique for the surface structural determination was applied to this disordered chlorine adsorbed on Ti (0001) surface. The diffuse scattering intensities were measured by a TV-computer method using a low light level video camera. From an analysis of two catalyst systems, the informations for the surface structure of the model catalyst surfaces were derived.

## Introduction

Ziegler-Natta catalyst is known as a catalyst which can polymerize olefins with very high activity and selectivity under a wide range of conditions. The catalytic phenomena was initially discovered by Ziegler based on the observation of an anormalous effect of an colloidal nickel on the Aufbau reaction[1] and this work was developed to the stereospecific polymerization of propylene and higher α-olefins[2] using titanium chloride by Natta.

Ziegler-Natta catalysts are generally formed by combining a metal alkyl or hydride, which is an activator, with a transition metal salt under an inert atmosphere.[3] The $TiCl_3/AlR_3$ system is a commercially used catalyst. Usually colloidal particles of α-$TiCl_3$ are disperced into the hydrocarbon solvent and then ethylene or propylene gas is bubbled through the mixture. The polymer forms rapidly around the surface of the finely disperced particles, entraining the catalyst and masking the initial stages of the reaction.

The stereospecificity which Ziegler-Natta catalyst shows in the olefin polymerization is usually explained by the interactions between nonbonded atoms at the catalytic site. Catalytic mechanism proposed by Cossee and Arlman[4~6] is most widely accepted and this is described by the coordination theory between α-olefin and titanium to the active center. However, the fundamental questions about the nature of the active sites still remained unsolved and hence the atomic structure of titanium/chloride surfaces should be understood precisely to identify active sites.

In this paper, I approached to this question to elucidate the nature of the titanium/chloride surfaces by two ways. One way was done with the $TiCl_3$ crystal itself. This is the direct method and has the advantage that we can study the real catalyst. On the other hand, it has some disadvantage that $TiCl_3$ crystals are very hard to work with, because they are only commercially available as very small crystalites and very water sensitive. The other way was done with an appropriate model catalyst system, which is an indirect method, to investigate such active sites. This strategy can be used to simulate a $TiCl_3$ surface under ultrahigh vacuum (UHV) condition, directly forming a chlorine layer on the Ti single crystal surface. This is a common approach due to the convenience and stability of the simulated sample. This model catalyst also has an advantage in that adsorbates can be isolated on a surface of known geometry.

In this study, both methods have been employed to understand the surface structures present in the titanium/chlorine system using the surface-sensitive techniques under ultrahigh vacuum condition.

## Experimental

**Preparation of Single Crystals.** Anhydrous, hydrogen-reduced, not-activated, powdered $TiCl_3$ (Alpha Products, U.S.A.) was used in growing $TiCl_3$ single crystals. A specially prepared pyrex tube, which can withstand a high temperature, was employed to grow $TiCl_3$ single crystals. The sample tubes had been stored in the drying oven at 130 ℃ and heated with a hot air gun before use. All manipulations of $TiCl_3$ crystals were carried out under Argon atmosphere in a dry box. The sample tube was vacuum sealed by an oxygen/acetylene torch and placed in the hot region of the gradient furnace. The gradient furnace which is used in sublimation and recrystallization of $TiCl_3$ crystals is shown in

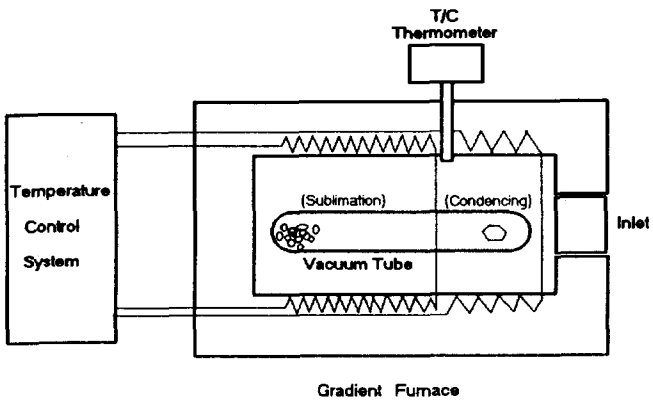


**Figure 1.** The design of electric gradient furnace used in growing single crystals.

Figure 1. Hot region in a gradient furnace is the sublimation portion, and the cold region is the condensing portion. Each portion of the furnace was consisted of a ceramic tube wound with nichrome wires for resistance heating. Two different sets of heating wires were regulated by the seperate variacs for the proper temperatures of each portion. The subliming portion of the tube was maintained at 480 to 495 ℃, and the condensing portion, at 380 to 390 ℃.[7] The vapor pressure was estimated to be about $2\times10^{-4}$ torr. Temperatures of the two regions in the furnace were checked periodically using the thermocouple (chromel/alumel) with which the furnace was equipped. It took about 5 days until $TiCl_3$ single crystal was formed from the sublimated vapor of $TiCl_3$ powder without seed. The shape of grown $TiCl_3$ single crystal was very thin leaflet-type crystal and 5 to 10 mm big in diameter and deep violet in color.

**Manipulation of Grown Single Crystals.** Since the grown $TiCl_3$ single crystal is very brittle and water-sensitive solid which is very difficult to work with, some special techniques were employed to prevent the crystal coming in touch with water vapor in the air until it was attached to the manipulator of the UHV chamber where it is to be studied. A vacuum deposition technique[8] was employed to protect the directly made single crystal from moisture in the air. Thin gold layer, which is employed as an inert layer, was formed on the crystal by vacuum deposition. The deposition apparatus used in this study was simply designed for gold-plating and made of pyrex. In this glass cell, tungsten ribbon which was spot-welded to the top of a tungsten welding rod was used as a heating template to vaporize gold and a gold wire (0.005″ Dia.) was coiled around the tungsten ribbon to be vaporized.

The freshly-grown $TiCl_3$ crystal was moved to the glass deposition cell in a dry box. The pressure of the vacuum cell was maintained to $2\times10^{-4}$ torr by a diffusion pump, and then the gold wire was heated and vaporized by the application of about 12 V AC and deposited on the $TiCl_3$ single crystal. Since the crystal was not hard enough to be clipped to the sample holder of the UHV chamber directly, as was a normal metal sample, special design was required to mount this brittle crystal. A molybdenum plate was employed as a template to be clipped to the manipulator. A thin indium film was sandwitched between the gold-plated

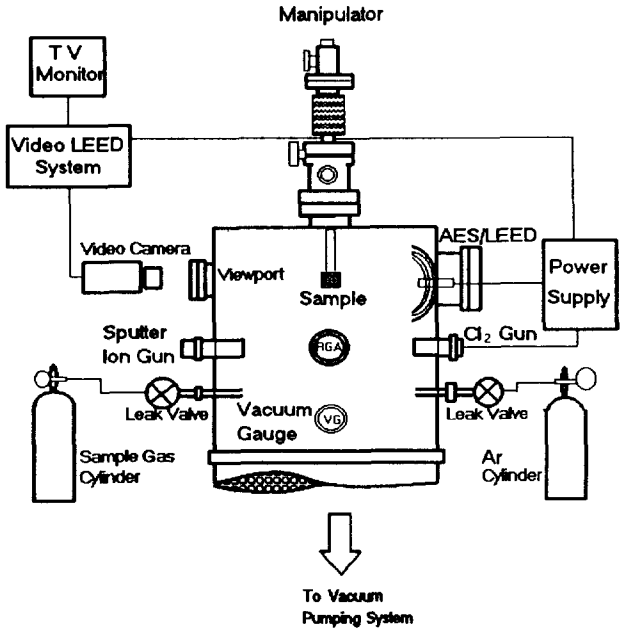


**Figure 2.** The schematic diagram of the UHV chamber used in experiments.

$TiCl_3$ crystal and the molybdenum plate. The molybdenum plate with the $TiCl_3$ crystal attached was then clipped to the sample holder which is attached to the manipulator of the vacuum chamber for UHV study.

**Preparation of Model Catalyst.** Titanium single crystal rod which is 99.999% pure and 1 inch long (Materials research coporation, Orangeburg, New York) was cut and oriented to the (0001) face using Laue back reflection technique.[8,9] The sample crystal was then polished by standard metallographic polishing methods.[10]

The sample was mounted to the sample holder in a manner which allows for heating and cooling by spot welding a tantalum heating wire around the outside edge of the disk-shaped crystal. A thermocouple was additionally spot welded to the unpolished back side of the sample to monitor the temperature of the sample.

After the sample holder was installed to the UHV chamber, *in-situ* cleaning was performed to the sample surface by Ar ion bombardment. Ar pressures of $5\times10^{-5}$ torr and a sample temperature of 600 ℃ was employed. The Ar ion beam energy and the sample current were set to 1 kV and 2.5 μA respectively. Usually Ar ion bombardments were carried out for 30 minutes, then the chamber was pumped down. Many cycles of this procedure eventually produced a surface without impurities except for the small amounts of carbon.

A molecular chlorine source, which is actually solid state electrochemical cell, was constructed and installed in the vacuum chamber for the purpose of chlorine dosing to the sample surface.[11] The great advantage of this chlorine gun is in its ability to provide a high dosing level without a corresponding increase in the chamber background pressure. This aspect of the chlorine gun minimizes the corrosion of the vacuum chamber and other installed equipments and reduces wall adsorption effects.

**Experimental Set-up and Measurements.** The experiments were carried out in a standard stainless steel UHV chamber, equipped with nine ion pumps in the lowest portion along with a titanium sublimation pump (TSP). The UHV chamber was equipped with four grid LEED optics which also functioned as an Auger spectrometer. In addition, the chamber was equipped with a quadrupole mass spectrometer (Dycor M200), an Ar ion sputter gun and a nude ionization gauge for pressure measurement. A diagram of the UHV chamber showing the locations of the various devices which were used in the experiments is illustrated in Figure 2. The base pressure of the chamber was maintained at below $2\times 10^{-10}$ torr. Auger, LEED and diffuse LEED experiments were carried out in this UHV chamber.

For UHV studies, a fast and sensitive data acquisition system is very important since residual gas adsorption may occur and contribute to the diffuse background for long measuring time. These requirements can be satisfied by employing video-based TV computer method using an image intensifier camera which can collect the weak diffuse intensities. The TV computer system consists of a low-light video camera (Cohu 5000 series), a video monitor, a video data acquisition card (Coreco Oculus 200+image analysis software) including fast video memory, and a processing computer which controls data acquisition, data handling, and the production of 3-D plots.

For the DLEED data collection, the diffuse intensity map including 4 LEED spots, the (0, 0), (1, 0), (0, 1) and (1, −1), was obtained and video images of the electronic window defined were averaged to reduce the experimental noise. All measurements were performed at normal incidence to the primary electron beam. The primary current was about 0.5 μA and the acceleration voltage onto the screen was about 3-4 kV. The diffuse intensities were measured in the range of 70 to 110 eV at 4 eV interval.

In order to determine the adsorption site and the structural parameters, the experimental data should be modeled using a theory which describes diffuse electron scattering from a disordered adsorbate on the surface at low coverages. A series of theoretical data was calculated by the theory based on the four possible adsorption sites and the assumed geometry. In this study, the program package which was developed by Van Hove and recently modified by Wander was used to calculate the diffuse intensities for a given local geometry. Then the calculated data were compared with the experimental data via the Pendry R-factor ($R_p$) to derive the proper geometry.

## Results and Discussion

**Auger Data for the $TiCl_3$ Crystals.** The Auger spectra were recorded for both gold plated and clean $TiCl_3$ crystal after the gold layer was removed by Ar ion sputtering. These spectra are shown in Figure 3.

For the gold plated surface, Auger peaks which are characteristic of gold appeared at 150, 160, 184 and 239 eV and the indium peak appeared at 404 eV. Carbon and oxygen are also found at 273 and 513 eV, respectively on the gold plated surfaces of $TiCl_3$. Titanium and chlorine peaks were not observed, which indicates that the gold-layer was thick enough to prevent the escape of Auger electrons from the

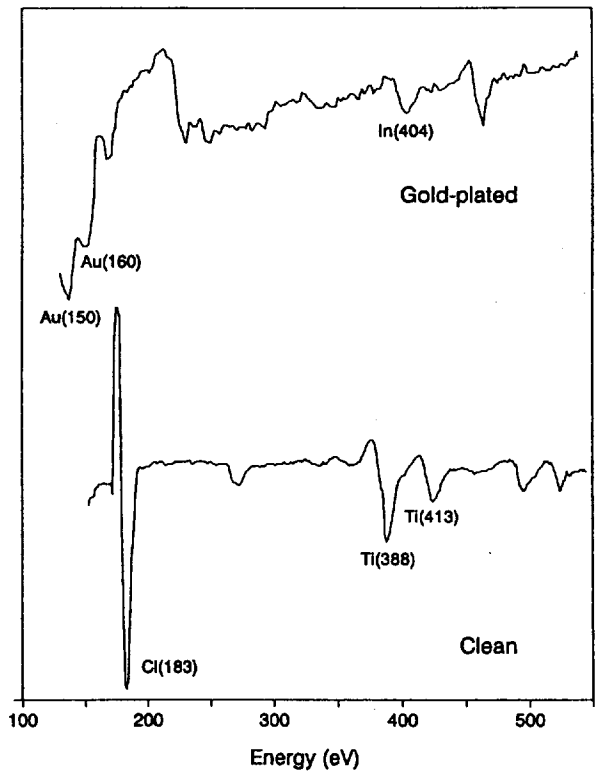


**Figure 3.** Auger spectra for the various states of $TiCl_3$ crystal (a) gold-plated (b) clean.

$TiCl_3$ crystal. Then the gold layer was removed by repeated Ar ion bombardments. The Auger spectrum for the clean $TiCl_3$ surface after removal of the gold layer is shown in the bottom of Figure 3. Gold peaks were not found on the spectrum any more and sharp titanium and chlorine peaks appeared at 388, 419 and 183 eV respectively, which indicates the $TiCl_3$ crystal surface was reproduced in the UHV chamber.

**LEED Pattern of the Clean $TiCl_3$ Crystal.** I attempted to observe the LEED pattern after following the cleaning procedure. The $TiCl_3$ crystal was annealed to repair the damaged surface caused by the repeated Ar ion bombardments. The annealing of the crystal was carried out both with and without the application of a chlorine flux to saturate the surface with chlorine while heating at 165 ℃ for overnight. The LEED pattern which was checked after annealing was not very good except for an increase in the diffuse scattered background.

This diffuse LEED pattern might be influenced by the two following reasons; a damaged surface by Ar ion beam during removal of the gold layer might not be recovered, which would result in disordered crystal surface; low annealing temperature which was not sufficiently high enough to repair the damaged surface. The annealing temperature could not be raised up above 165 ℃ because of the low melting point (176 ℃) and high volatility of indium, even though a good annealing temperature was thought to be higher than this. Actually a small indium peak was found in the Auger spectrum of the $TiCl_3$ crystal that had been annealed overnight. This indicated that some indium might have been evaporated. On the other hand, I can not exclude the possi-

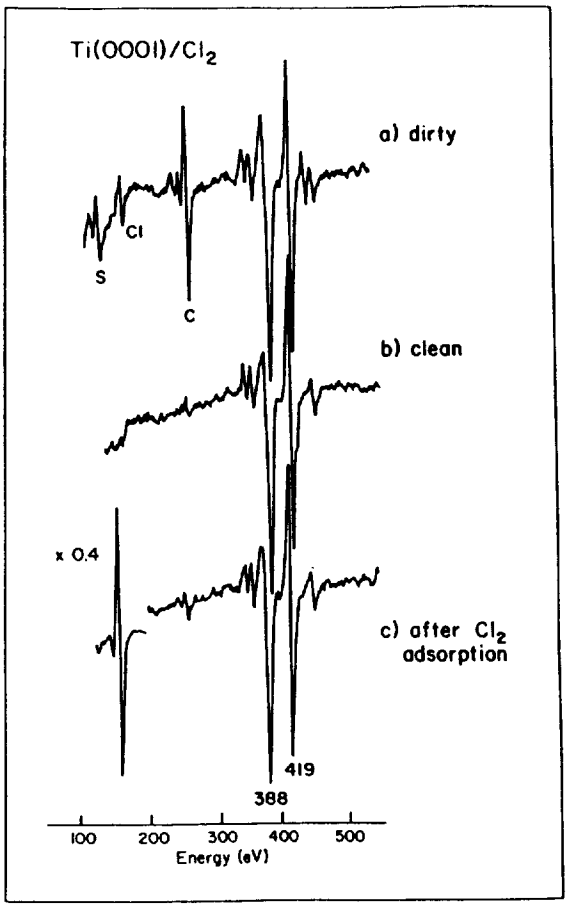


**Figure 4.** Auger spectra (1 keV, 20A) of the Ti (0001) surface (a) contaminated, (b) clean, and (c) after a saturation exposure of chlorine.

bility that the original surface of the $TiCl_3$ crystal might be disordered, which unables the observation of good LEED pattern.

These results, the failure of the regular LEED technique on the real catalyst, required me to employ another technique which allows surface structural studies on the disordered surface.

**Auger and LEED Results for the Model Catalyst.** It was possible to distinguish the differences between the Auger spectra of dirty, clean, and chlorine-covered titanium surfaces. Significant amounts of carbon, sulfur and chlorine impurities were shown for the initial Auger spectrum of the sample in Figure 4. These impurities showed characteristic peaks at 271, 154 and 183 eV, respectively. I could reduce these impurities to the level of 1% by many cycles of Ar ion sputtering at high temperature (650 ℃) and thermal flashes to 700 ℃ for about 20 seconds.

The Ti (0001) surface was dosed with chlorine by using the solid state electrochemical source.[11] The dose of chlorine was measured in microcoulombs of cell current, based on Faraday's law. Typical Auger spectra for the chlorine saturated Ti (0001) surface, taken after by a chlorine dose of 5000 μC was shown in Figure 4. The uptake curve of the chlorine on the Ti (0001) surface was determined by measuring the change in the chlorine (183) Auger peak height after successive doses with chlorine were applied to the surface.

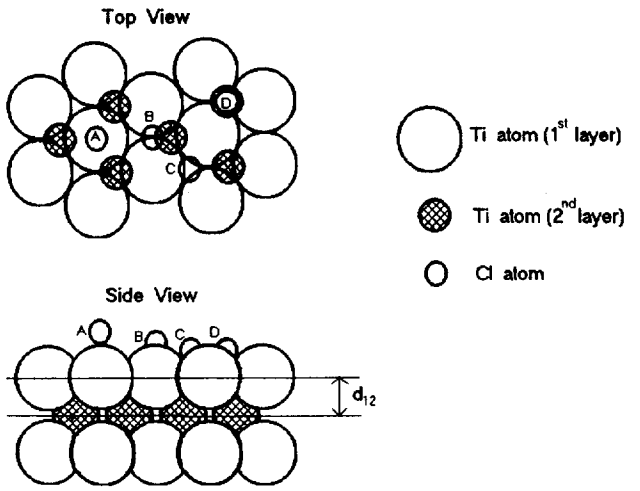


**Figure 5.** Four different adsorption sites of chlorine atoms on Ti (0001) surface.

At saturation exposure, a value for the ratio of Auger signals of Cl (183)/Ti (388) was found to be 7.12± 0.2 which reasonably agrees with the value of 9.1 of Smith[12] measured using a similar retarding field analyzer.

After sample cleaning, the typical six-fold symmetric diffraction pattern for the Ti (001) surface was observed. The LEED pattern observed after the passage of 250 μC of charge passed through the Cl dosing cell did not show any change from the hexagonal pattern of the clean Ti (0001) surface. This corresponded to a Cl coverage of about 20% of a monolayer based on the uptake curve. It was observed that the only diffuse background increased on the chlorine covered Ti (0001) surface, in comparison with the clean surface. This is in agreement with the results of a previous study reported by Dr. Watson's group.[13] It was found that an ordered LEED pattern of Cl could be only observed after heating a Cl saturated surface at temperatures of up to 650 ℃ for the period of 5 to 30 minutes. This result indicates that the chlorine atoms adsorbed on Ti (0001) surface with low coverage and at room temperature are disordered.

**DLEED Results.** For comparison with experiment, it was assumed that chlorine atoms would probably adsorb on 4 different possible sites on the Ti (0001) surface, those are ontop, bridge, 3-fold hollow with no atom under (**3fn**), and 3-fold hollow with an atom under (**3fa**) sites. The positions of relative adsorption site are demonstrated in Figure 5. The atomic radii of Ti and Cl atoms are 1.47 Å and 1.81 Å, respectively. The *x*, *y* and *z* coordinate values for the possible positions of Cl atoms adsorbed on the first Ti layer are; A (ontop)=(0, 0, 3.28), B (bridged)=(2.5548, 0, 2.932), C (**3fn**) =(1.7032, 0, 2.8056), D (**3fa**)=(−1.7032, 0, 2.8056). The distances between the first titanium layer and the chlorine adsorbates were varied within a reasonable range about the values obtained from hard sphere models. For each of the 4 different adsorption sites, theoretical diffuse intensities and Y-functions were calculated from 11 to 18 Ti-Cl distances, in a range of 2.15 to 3.43 Å in 0.05 Å increments for each of the corresponding geometries. It was assumed that the symmetry of the substrate is not distorted by adsorption of 20% of a monolayer of chlorine and that no reconstruction occurs.

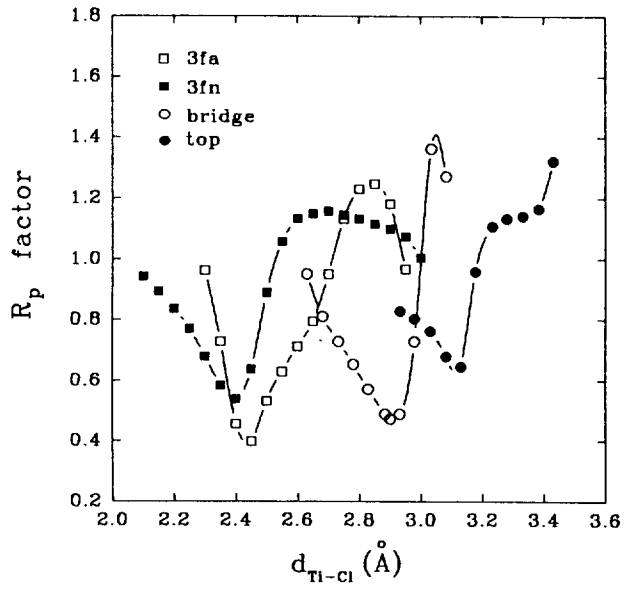


**Figure 6.** Pendry R-factor analysis of experimental data taken at 78/82 eV, (20% ML, 173 K) and theoretical calculations for 4 different adsorption sites.

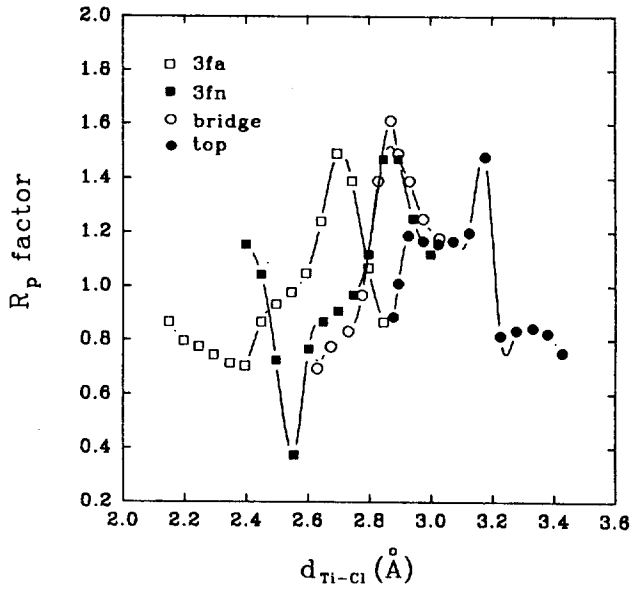


**Figure 7.** Pendry R-factor analysis of experimental data taken at 90/94 eV, (20% ML, 173 K) and theoretical calculations for 4 different adsorption sites.

**Table 1.** Results of an R-factor Analysis for Cl/Ti (0001) at 0.2-ML Coverage, 173 K, 78/82 eV Energy Pair. Here **3Fa** Indicates a 3-fold Site with an Adjacent Atom in the Layer Underneath and **3Fn** Indicates a 3-fold Site with No Atom Underneath

| Site | $R_p$ (min) | $d_{Ti-Cl}$(min) (Å) | Ti-Cl bond length (Å) |
|---|---|---|---|
| A-1F | 0.649 | 3.13 | 3.13 |
| B-2F | 0.471 | 2.90 | 3.25 |
| C-3Fa | 0.405 | 2.45 | 2.98 |
| D-3Fn | 0.536 | 2.40 | 2.94 |

**Table 2.** Results of an R-factor Analysis for Cl/Ti (0001) at 0.2-ML Coverage, 173 K, 90/94 eV Energy Pair. Here **3Fa** Indicates a 3-fold Site with an Adjacent Atom in the Layer Underneath and **3Fn** Indicates a 3-fold Site with No Atom Underneath

| Site | $R_p$ (min) | $d_{Ti-Cl}$(min) (Å) | Ti-Cl bond length (Å) |
|---|---|---|---|
| A-1F | ...* | ... | ... |
| B-2F | ...* | ... | ... |
| C-3Fa | 0.732 | 2.40 | 2.94 |
| D-3Fn | 0.376 | 2.55 | 3.06 |

*No minimum was found.

For the calculations of the diffuse intensities at the energies of 78 and 82 eV, the values of the vertical distance of the chlorine atom to the first Ti layer ($d_{Ti-Cl}$) was varied in steps of 0.05 Å. Experimentally, the Ti (0001) surface always appears to exhibit 6-fold symmetry resulting from surface termination by equal amounts of domains of the two terminations.[14] Therefore, two seperate calculations were carried out for each termination. The calculated intensity values were averaged and subsequently used to calculate the Y-functions[15] for comparison with the experimental data.

From the LEED theory, the real part of the optical potential experienced by an electron that enters solid, so called "inner potential ($V_{or}$)", is a priori unknown quantity. In the calculation, this was set to a reasonable value of $-10$ eV, but it is possible that this value may be in error by up to several eV. The result of such an error ($\Delta V_{or}$) would be that the experimental data taken at $V$ eV should be compared with a calculation performed at $V+V_{or}$ eV rather than at $V$ eV itself. To avoid this theoretical problem, several sets of calculations using neighboring energies for a given experimental energy were carried out. The best fit between the experimental data and the theoretical calculations was determined, which corresponds to the lowest value of $R_p$. In our calculations, It was appeared that the theoretical data calculated for the same energy (78/82 eV) as the experimental data provide the best agreement.

Detailed analysis for the different adsorption geometries was made using the Pendry R-factor ($R_p$) between the experimental and the calculated Y-functions. This analysis enables us to discriminate the unfavored sites among them and provide an unequivocal determination of structural parameters. The results of this analysis for **4** different adsorption sites are shown in Figure 6 and gathered in Table 1. The plot shows the value of $R_p$ for the **4** adsorption sites under consideration, at various values of $d_{Ti-Cl}$. All four sites show clear minima in the R-factor analysis. The on-top site (A) is clearly unfavored. The bridge site (B) shows poorer agreement with experiment than the **3** fold sites (C, D). The two 3-fold hollow sites show a minimum R-factor at almost the same interlayer seperation, with the (C) site showing a better agreement with experiment.

Another set of analysis was repeated for the data at the 90/94 eV energy pair. The results of Pendry R-factor analysis

are shown in Figure 7 and Table 2. It is shown that only the 3fn site has a clear minimum (2.55 Å). The **3fa** site shows a broad minimum around the same $d_{Ti-Cl}$ value seen for the 78/82 eV data set (2.40-2.45 Å). For the 90/94 eV data, the on-top and bridge sites show no reasonable minima.

I also tried to analyze experimental data for different chlorine coverages (10 and 40% of a monolayer). For 10% of a monolayer, the diffuse intensities were not large enough to analyze; for 40% of a monolayer, the analysis was disturbed by the partial ordering due to adsorbate-adsorbate interaction.

The results from both datasets point to the adsorption site for Cl on Ti (0001) being a 3-fold hollow site. Unfortunately, the two sets of data differ in the site that produces the best agreement. In one case (78/82 eV) the best agreement is with the **3fa** site that has an atom underneath (site C). For the other dataset (90/94 eV), best agreement is with the **3fn** site that has no adjacent atom in the layer underneath (site D). It shows that it has some difficulty in distinguishing them on the small difference in the nature of these two adsorption sites. I can take a conventional approach by reporting the adsorption site as a 3-fold hollow site with a Ti-Cl interlayer spacing of 2.48± 0.07 Å and a Ti-Cl bond length of 2.96± 0.02 Å, where the error bar covers the range of values encountered in both datasets.

The best R-factor value of about 0.4 obtained here is in moderately good agreement, being poorer that the value of 0.13 obtained in the DLEED study of O/W (100) by Heinz *et al.*,[16] but better than the value of 0.55 obtained by Blackman et al for CO/Pt (111).[17]

It is interesting to enquire how this experimental result fits into solid state consideration to rationalize trends in adsorption sites and bond lengths for atomic adsorption on metal surfaces. Mitchell[18,19] has discussed some approaches for assessing the near neighbor *X-M* interatomic distances when main group (*X*) atoms are chemisorped on crystallographically well-defined surfaces of metals (*M*). One promising method for predicting surface bond distances is to use bond valence-bond length relationships deduced from an analysis of solid state structures by Brown and Altermatt.[20] The Brown-Altermatt method, as modified by Mitchell, uses the expression:

$$r = r_o - 0.85 \log S$$

for a particular interatomic distance $r$. In this equation $r$ depends on the bond valence of the $S$, and $r_o$, which is the corresponding distance for a bond of unit valence in a suitable solid. The use of this equation requires the assumption that the sum of the bond valences for each $X$ atom equals the atomic valence $v$. In this case where $X$ adsorbs on a metallic surface with $n$ equivalent neighboring $M$ atoms, the bond valence equals $v/n$. To find the Ti-Cl surface bond length predicted by this formula, $TiCl_2$ was taken as a reference compound, perhaps the closest solid-state analog to the Cl/Ti (0001) adsorption system for which crystallographic information is available, the Ti-Cl distance is 2.53 Å. When this value was chosen as a reference value $r_o$, the bond length of 2.94 Å for adsorption of Cl in the 3-fold surface sites on Ti (0001) was predicted. This result showed very good agreement between this predicted value of 2.94 Å and the experimentally-determined value of 2.96 Å.

## Conclusion

The simple and convenient process that manipulates the air-sensitive and fragile single crystals for the UHV study has been developed and applied to $TiCl_3$ single crystal that is the real catalyst of Ziegler-Natta catalyst system. This process was verified by AES. Diffuse LEED pattern observed for the $TiCl_3$ surface indicates that the $TiCl_3$ single crystal surface might be disordered, even though it was not enough to make a conclusion.

DLEED intensities from 0.2 ML of atomic chlorine adsorbed at 173K on Ti (0001) surface which was a model system of the Ziegler-Natta catalyst have been measured. From the results of R-factor analysis for the Y-functions at 78/82 and 90/94 eV, the best fit value resulted that Cl atom adsorbed in a **3** fold hollow site on the Ti surface with a Ti-Cl interlayer spacing of 2.48± 0.07 Å. The surface bond length of Ti-Cl was estimated to be 2.96 Å based on this result. This results is in good agreement with the value of 2.94 Å predicted by theoretical considerations.

## References

1. Ziegler, K.; Holzcamp, E.; Breil, H.; Martin, H. *Angew. Chem.* **1955**, *67*, 541.
2. Natta, G. *J. Polymer Sci.* **1955**, *16*, 143.
3. Gaylord, N. G.; Mark, H. F. *Linear and Stereoregular Addition Polymers*; Interscience: New York.
4. Arlman, E. J. *J. Catalysis* **1964**, *3*, 89.
5. Arlman, E. J.; Cossee, P. *J. Catalysis* **1964**, *3*, 99.
6. Novaro, O.; Chow, S.; Magnouat, P. *J. Catalysis* **1976**, *41*, 91.
7. Canadine, Jr., W. R.; Rase, H. F. *J. Appl. Polymer Sci.* **1971**, *15*, 889.
8. Preuss, E. *Laue Atlas*; John Wiely & Sons: New York, London, Toronto.
9. Wood, E. A. *Crystal Orientation Manual*; Columbia University Press: New York and London, 1963.
10. American Society for Metals, *Metal Handbook*; Cleveland: Ohio, 1948.
11. Spencer, N. D.; Goddard, P. J. *J. Vac. Sci. Technol.* **1983**, *A1*, 1554.
12. Smith, T. *J. Electrochem. Soc.* **1972**, *119*, 1398.
13. Watson, P. R.; Mokler, S. M.; Mischenko III, J. *J. Vac. Sci. Technol. A*, **1988**, *6*(3), 671.
14. Davis, H. L.; Zehner, D. M. *J. Vac. Sci. Technol.* **1980**, *17*(1).
15. Pendry, J. B. *J. Phy. Chem.* **1980**, *13*, 937.
16. Heinz, K.; Saldin, D. K.; Pendry, J. B. *Phy. Rev. Lett.* **1985**, *55*, 2312.
17. Blackman, G. S.; Ogletree, D. F.; Van Hove, M. A.; Somorjai, G. A. *Phy. Rev. Lett.* **1988**, *61*, 2352.
18. Mitchell, K. A. *R. Surface Sci.* **1985**, *143*, 93.
19. Mitchell, K. A. R.; Schlatter, S. A.; Sodhi, R. N. S. *Can. J. Chem.* **1986**, *64*, 1435.
20. Brown, I. D.; Altermatt. *Acta Crystallgr.* **1985**, *B41*, 244.